Journal of Low Temperature Physics, Vol. 33, Nos. 5/6, 1978

Suppression of *P*-Wave Superfluidity in Long, Narrow Pores

L. H. Kjäldman and J. Kurkijärvi

Department of Technical Physics and Low Temperature Laboratory, Helsinki University of Technology, Espoo, Finland

and D. Rainer

Institut für Festkörperforschung der Kernforschungsanlage Jülich, Jülich, Germany

(Received June 12, 1978)

The transition temperature of superfluid ^{3}He is calculated as a function of the size of an infinitely long cylindrical pore or an infinite slab container with diffusely scattering walls. We present the exact asymptotic behavior for large and small containers and a full numerical calculation for intermediate sizes.

1. INTRODUCTION

P-wave superfluids are strikingly different from *s*-wave superfluids in that ordinary scattering from walls or any foreign object can lead to local suppression of the order parameter.[1] A large density of foreign objects or confinement to a limited space is likely to reduce the transition temperature and finally eliminate the transition altogether. For regular enough container shape the scattering boundary condition plays an important role in this context. This fact could eventually be used to investigate the scattering properties of surfaces.

We investigate quantitatively the lowering of the superfluid transition temperature of ^{3}He as a function of the size of the system in two simple geometries, the infinitely long cylindrical pore and the infinite slab with diffusely scattering boundaries. Both these geometries have the property that the transition temperature should remain unchanged and there should be no critical smallest size for the superfluid transition to occur if the walls reflect specularly. A measurement of the transition temperature in either of these geometries should therefore bring direct information on the degree of diffusiveness of the surface scattering.

0022-2291/78/1200-0577$05.00/0

The next obvious simple geometry, the sphere, seems a much more complicated problem and we have not treated it. In addition to the wall effects in the sense of the present paper, there is the texture problem in a sphere. As there is no direction for a conserved current in a sphere, specular scattering alone can lead to suppression of the order parameter in a spherical container. One should therefore exercise some care in applying the present quantitative results to other than geometries that reasonably may be described as pores or slabs.

Another interesting application of the present results could be in the design of an experiment looking for an ordinary "external" Josephson effect in ^{3}He. The fact that the order parameter is reduced in a pore may essentially improve the chance for observing such an effect in ^{3}He, as the coupling strength may be controlled with the temperature.

There are several known experimental studies of ^{3}He in confined geometries where no transition to the superfluid phase has been observed. To our knowledge, however, no systematic investigation of the size effect has taken place.[2]

Previous theoretical studies of ^{3}He in slabs or cylinders concentrate on textures and are restricted to large sizes compared with the coherence length. In all of them use is made of the Ginzburg–Landau expansion[3] or of a long-wavelength hydrodynamic approach.[4] We are interested in size effects on the scale of the coherence length $\xi_0 \simeq 150$ Å. This requires that we include nonlocal effects in our analysis.

In this paper we present numerical results on the critical temperature of a narrow cylinder (slab) for all radii as well as analytic treatments of the two asymptotic limits: the case of large radius and the case of small deviations from the critical radius where the transition temperature goes to zero. We find the critical sizes $R_c = 1.5\xi_0$ for a pore and $D_c = 1.3\xi_0$ for a slab.

In Section 2 we give the theoretical background for the integral equation that determines the transition temperature as a function of the size of the system. The asymptotic solutions are discussed in Sections 3 and 4 and the numerical results in Section 5. All these results are summarized in Figs. 2 and 3.

2. TECHNICAL DETAILS

We are interested in the lowering of the superfluid transition temperature of ^{3}He in finite containers brought about by the pair-breaking effect of the walls. No reliable theory for calculating the bulk (infinite-system) transition temperature T_c^0 itself is available,[5] as T_c^0 depends on unknown high-energy structures of the excitation spectrum of ^{3}He. In contrast, the change in the transition temperature is determined by the low-energy excitations, the quasiparticle part of the spectrum. It can be calculated with

the theory, correct in the weak coupling limit ($T_c^0/E_F \to 0$), developed in Ref. 6. T_c is determined by the linearized gap equation

$$A_{si}(\mathbf{r}) = \sum_j \int d^3r'\, K_{ij}(\mathbf{r}, \mathbf{r}') A_{sj}(\mathbf{r}') \tag{1}$$

$$K_{ij}(\mathbf{r}, \mathbf{r}') = 6\pi N(0) g T \sum_n{}' \int_0^\infty dt \exp(-2|\varepsilon_n|t) \times (1/v_F^2)\langle j_i(\mathbf{r}, 0) j_j(\mathbf{r}', t)\rangle_{\text{classical}} \tag{2}$$

where $\langle j \cdot j\rangle_{\text{classical}}$ is the classical current–current correlation function in a microcanonical ensemble of particles with velocity v_F. The frequency sum over $\varepsilon_n = (2n-1)\pi T$ is cut off at an arbitrary energy $E_c \gg T_c^0$ and g is a pseudo coupling constant chosen to reproduce the correct bulk transition temperature. Any sensible result must be insensitive to the cutoff E_c, which can be eliminated according to the limiting procedure

$$\begin{matrix} E_c \to \infty \\ g \to 0 \end{matrix} \quad \text{such that} \quad T_c^0 = 1.13\, E_c \exp\left[-\frac{1}{N(0)g}\right] = \text{const}$$

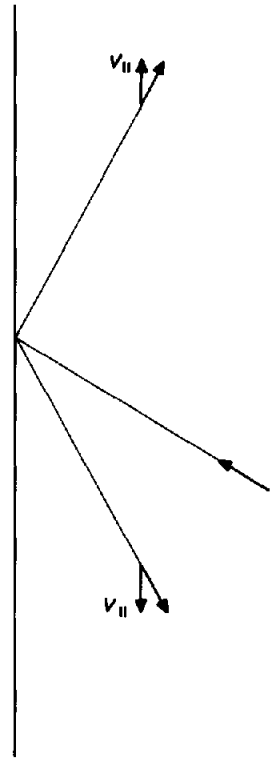

Fig. 1. Two reflected paths whose contributions to the kernel in the gap equation cancel each other. Both paths have the same length but end up with opposite velocity components along the wall.

The current–current correlation function and hence the kernel of the gap equation depend on the geometry of the container. The current–current correlation function, complicated to calculate in general, can be easily determined for a cylinder or a slab with diffusely scattering walls by the following considerations.

The equilibrium order parameter has in both cases only components parallel to the walls and these only vary as a function of distance from the walls, i.e., the radial coordinate of a cylinder or the z coordinate of a slab in the (x, y) plane. Hence only the current–current correlation function integrated over the coordinates parallel to the wall (z, ϕ for a cylinder; x, y for a slab) enter the gap equation. In the integrated correlation function of the velocity components along the walls only such correlations survive that result from direct propagation from one point to another; paths scattered by the diffusely scattering walls cancel each other pairwise as demonstrated in Fig. 1. To determine the transition temperature of a cylinder (slab), one only needs the free particle (bulk) correlation function. The effect of reduced transition temperature arises from the restrictions on the integration volume Ω as compared with the bulk case. We then have the bulk kernel

$$K_{ij}^{\text{bulk}}(\mathbf{r}, \mathbf{r}') = \frac{3N(0)gT}{2v_F} \sum_n{}' \frac{(\mathbf{r}-\mathbf{r}')_i (\mathbf{r}-\mathbf{r}')_j}{|\mathbf{r}-\mathbf{r}'|^4} \exp - \frac{2|\varepsilon_n||\mathbf{r}-\mathbf{r}'|}{v_F} \tag{3}$$

After integrations over the coordinates parallel to the wall one finds the one-dimensional integral equations for radial dependence of the order parameter in the pore (z dependence in a slab, respectively)

$$\lambda A_{sz}(r) = \int_0^{\bar{R}} dr'\, k^{\text{pore}}(r, r') A_{sz}(r') \tag{4}$$

$$\lambda A_{s\parallel}(z) = \int_{-\bar{D}/2}^{+\bar{D}/2} dz'\, k^{\text{slab}}(z-z') A_{s\parallel}(z') \tag{5}$$

where $\lambda = 4/3N(0)g$, and

$$k^{\text{pore}}(r, r') = \frac{2}{\pi} r' \sum_{n=1}^{N} \int_0^{2\pi} d\phi \int_{-\infty}^{+\infty} d\eta\, \eta^2 \times \frac{\exp\{-(2n-1)(r^2+(r')^2-2rr'\cos\phi+\eta^2)^{1/2}\}}{[r^2+(r')^2-2rr'\cos\phi+\eta^2]^2} \tag{6}$$

$$k^{\text{slab}}(z-z') = 2 \sum_{n=1}^{N} \{E_1[(2n-1)|z-z'|] - E_3[(2n-1)|z-z'|]\} \tag{7}$$

and all lengths are expressed in units of the coherence length $v_F/2\pi T$.

One obtains the size-dependent transition temperature from the largest eigenvalue λ in the following parametric representation:

$$T_c/T_c^0 = \exp\left(\tfrac{3}{4}\lambda\right)/1.13\pi(2N-1) \tag{8a}$$

$$R/\xi_0 = 1.13(2N-1)\bar{R}\exp\left(-\tfrac{3}{4}\lambda\right) \tag{8b}$$

R is the radius of the pore and $T_c = T_c(R)$ is its transition temperature. N and $\bar{R}$ are parameters in the eigenvalue problem (4). The corresponding parametric representation of $T_c(D)$ for a slab is simply obtained by replacing R ($\bar{R}$) in (8b) by D ($\bar{D}$) and using λ from Eq. (5).

Equations (4)–(8) still contain the cutoff energy E_c and the pseudo coupling constant g. It was convenient for the calculations of Section 5 to keep this spurious cutoff dependence in the numerical algorithm. The final results were made practically cutoff-independent by choosing a large enough cutoff. The numerical analysis of Section 5 is based on the gap equations (4) and (5) with the kernels specified by (6) and (7). The analytical results of Sections 3 and 4, on the other hand, are based on a cutoff-independent version of the gap equation. In order to eliminate the cutoff we have to write the gap equation (1) in the unconventional form

$$\sum_j \left[\delta_{ij} - \int d^3r'\, K_{ij}(\mathbf{r}, \mathbf{r}')\right] A_{sj}(\mathbf{r})$$

$$= \sum_j \int d^3r'\, K_{ij}(\mathbf{r}, \mathbf{r}')[A_{sj}(\mathbf{r}') - A_{sj}(\mathbf{r})] \tag{9}$$

The limit $E_c \to \infty$ is now trivial on the right-hand side since the singularity of the kernel at $\mathbf{r} = \mathbf{r}'$ is cancelled by the vanishing factor $A_{sj}(\mathbf{r}') - A_{sj}(\mathbf{r})$. We are left with an integral equation of the form [we have taken the bulk kernel, Eq. (3)]

$$\sum_j \phi_{ij}(\mathbf{r}, T) A_{sj}(\mathbf{r})$$

$$= \sum_j \int_\Omega d^3r' \frac{(\mathbf{r}-\mathbf{r}')_i(\mathbf{r}-\mathbf{r}')_j}{|\mathbf{r}-\mathbf{r}'|^4}$$

$$\times \frac{3T/2v_F}{\sinh(2\pi T|\mathbf{r}-\mathbf{r}'|/v_F)}[A_{sj}(\mathbf{r}') - A_{sj}(\mathbf{r})] \tag{10}$$

where the function $\phi_{ij}(\mathbf{r}, T)$ is given as the $E_c \to \infty$ limit of the following expression:

$$\phi_{ij}(\mathbf{r}, T) = \lim_{E_c \to \infty;\, g \to 0} \left\{ \frac{\delta_{ij}}{N(0)g} - \frac{3T}{2v_F} \sum_n{}' \int_\Omega d^3 r' \times \frac{(\mathbf{r}-\mathbf{r}')_i (\mathbf{r}-\mathbf{r}')_j}{|\mathbf{r}-\mathbf{r}'|^4} \exp - \frac{2|\varepsilon_n| |\mathbf{r}-\mathbf{r}'|}{v_F} \right\} \tag{11}$$

We note that this integral is independent of the order parameter. It does depend, however, on the geometry of the container. The low-temperature limit of $\phi_{ij}(\mathbf{r}, T)$ can be found analytically for cylindrical and slab geometries:

$$\phi_{zz}^{\text{pore}}(r, T=0) = -\left(\log \frac{R}{4\xi_0} + \frac{4}{3} + \frac{1}{2} \log \frac{R^2 - r^2}{R^2} \right) \tag{12a}$$

$$\phi_{xx}^{\text{slab}}(z, T=0) = -\left(\log \frac{D}{4\xi_0} + \frac{4}{3} + \frac{1}{2} \log \frac{D^2 - 4z^2}{D^2} \right) \tag{12b}$$

The cutoff-independent gap equation (10) is used in Section 4 to calculate the critical size below which superfluidity is absent in a pore or a slab.

3. GINZBURG–LANDAU LIMIT

At large radius of the cylinder the order parameter varies slowly compared with the range of the kernel in (1). One may then use a local

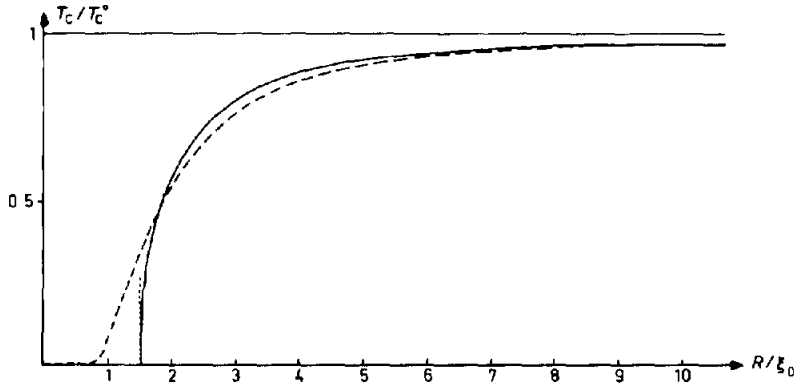

Fig. 2. Transition temperature as a function of the radius R in a cylindrical pore with diffusely scattering walls. The asymptotic results in the Ginzburg–Landau range and near the critical pore size are given as a dashed line and a dotted line, the full numerical result as a solid line.

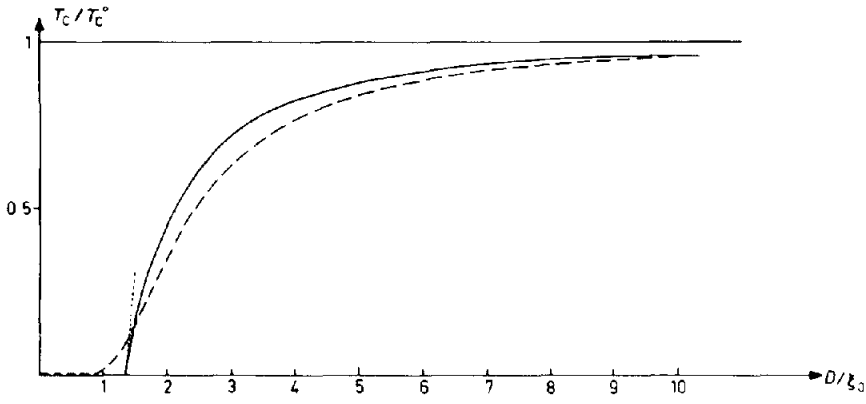

Fig. 3. Transition temperature as a function of the thickness D in a slab between diffusely scattering planes. The asymptotic results in the Ginzburg–Landau range and near the critical thickness are given as a dashed line and a dotted line, the full numerical result as a solid line.

approximation for the kernel, which leads to the Ginzburg-Landau equation

$$\log \frac{T_c^0}{T_c} A_{si}(\mathbf{r}) + \frac{3}{5}\xi_s^2 \sum_j (\delta_{ij}\nabla^2 + 2\nabla_i\nabla_j) A_{sj}(\mathbf{r}) = 0 \tag{13a}$$

$$\xi_s^2 = 7v_F^2\zeta(3)/[48\pi^2(T_c^0)^2]$$

together with the boundary condition

$$A_{sj}(\mathbf{r} \text{ at boundary}) = 0 \tag{13b}$$

These equations (including third-order terms in the order parameter on external perturbations) have been discussed by several authors for the slab as well as the cylinder geometries.[4] They can be easily solved and yield the size-dependent transition temperatures

$$T_c = T_c^0 \exp(-\tfrac{3}{5}\xi_s^2\alpha^2/R^2) \qquad \text{(pore)} \tag{14a}$$

for a cylinder of radius R and

$$T_c = T_c^0 \exp(-\tfrac{3}{5}\xi_s^2\pi^2/D^2) \qquad \text{(slab)} \tag{14b}$$

for a slab of thickness D, where $\alpha = 2.4048$ is the first zero of the Bessel function $J_0(x)$. They are shown in Figs. 2 and 3 together with exact numerical results, with which they agree reasonably down to a pore size of the order of $R/\xi_0 = 5$ (slab thickness $D/\xi_0 = 6$). At smaller sizes, however, they give too high superfluid transition temperatures and do not lead to finite critical sizes. To pin down the lower end of the curve we now turn to the low critical temperature limit.

4. CRITICAL SIZES

The transition temperature to the superfluid phase goes to zero at a critical size below which the system no longer becomes superfluid at all. In contrast to the Ginzburg–Landau limit, the sample dimensions here are much smaller than the coherence length $\xi = v_F/2\pi T_c$. We therefore look for the smallest radius that gives a nonvanishing solution of the gap equation taken at $T = 0$. It is convenient to start with Eq. (10), where the cutoff E_c and the pseudo coupling constant of the conventional gap equation (1) have been eliminated in favor of the bulk transition temperature. Taking the limit $T = 0$ and integrating over those spatial variable components that do not appear in the order parameter, we find the parameterless eigenvalue equations

$$E_{\text{pore}}\bar{\Delta}(\rho) = \log(1-\rho)\bar{\Delta}(\rho) + \int_0^{+1} d\rho' \frac{1}{|\rho'-\rho|}[\bar{\Delta}(\rho') - \bar{\Delta}(\rho)] \tag{15a}$$

$$E_{\text{slab}}\bar{\Delta}(\zeta) = \log(1-\zeta^2)\bar{\Delta}(\zeta) + \int_{-1}^{+1} d\zeta \frac{1}{|\zeta-\zeta'|}[\bar{\Delta}(\zeta') - \bar{\Delta}(\zeta)] \tag{15b}$$

The eigenvalues E_{pore} and E_{slab} determine the critical sizes R_c and D_c through the relations

$$R_c = 4\xi_0 \exp(-\tfrac{1}{2}E_{\text{pore}} - \tfrac{4}{3}) \tag{16a}$$

$$D_c = 4\xi_0 \exp(-\tfrac{1}{2}E_{\text{slab}} - \tfrac{4}{3}) \tag{16b}$$

We calculated the eigenvalues with standard computer routines, using two different expansions for the eigenfunctions, an expansion in terms of Legendre polynomials and an expansion in terms of piecewise constant functions. We find $E_{\text{pore}} = -0.71$ and $E_{\text{slab}} = -0.47$ and critical sizes

$$R_c = 1.5\xi_0 \tag{17a}$$

$$D_c = 1.3\xi_0 \tag{17b}$$

The profile of the amplitude of the order parameter near the critical size is shown in Fig. 4. It is also interesting to determine how the critical temperature departs from zero as a function of $R - R_c$ or $D - D_c$. This is determined by the leading finite-temperature corrections to Eqs. (15), which can be calculated from Eq. (10). In a pore the corrections take the form $T^2 \log T$, which implies that T_c starts with an infinite slope at the critical radius. For a slab the leading correction is linear in T and can be evaluated analytically. It results in a linear departure of T_c as a function of $D - D_c$:

$$\frac{D-D_c}{\xi_0} = \frac{D_c^2}{\xi_0^2}\frac{3\log 2}{4}\frac{T}{T_c} \simeq 0.92\frac{T}{T_c} \tag{18}$$

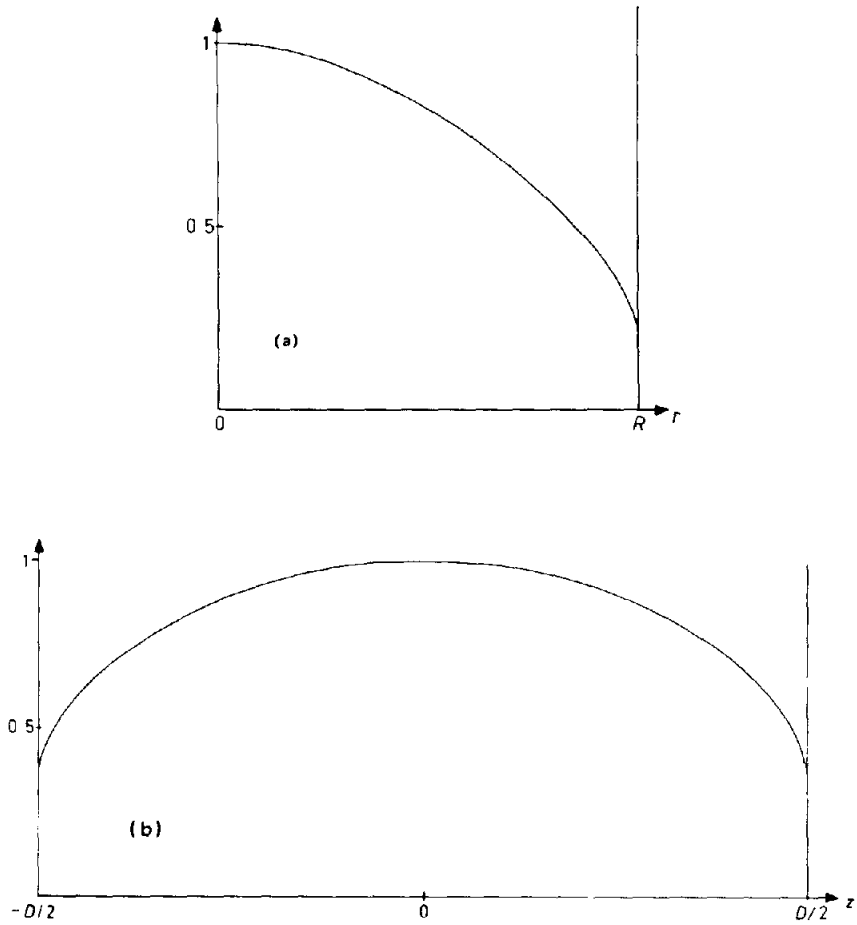

Fig. 4. Amplitude of the order parameter (a) in a pore and (b) in a slab, near the critical sizes normalized to 1 at the center and computed with a Legendre polynomial expansion (15 polynomials) for the order parameter. This approximation fails right at the wall, where the correct order parameter has an infinite slope.

The low-temperature behavior is also shown in Figs. 2 and 3, together with the numerical results for arbitrary sizes. One can see that the asymptotic results at large sizes on the one hand and at low critical temperatures on the other hand give a fairly well-defined idea about the size dependence of the transition temperature in pores and slabs with diffusely scattering walls. They also provide checks on the numerical treatment of the full integral equation necessary for further details.

5. NUMERICAL CALCULATION

In order to determine the transition temperature for other than the asymptotic limits one has to solve the gap equation numerically. It reduces to a one-dimensional integral equation for both the cylindrical pore and the slab. For the slab the kernel of the equation is explicitly known, whereas it is only given as a two-dimensional singular integral for the cylindrical pore. This makes the pore an essentially more difficult case than the slab. For the slab the integral equation can be transformed into a standard matrix equation by simply approximating the order parameter with piecewise linear functions. The matrix elements can be evaluated analytically and the matrix equation solved with library routines. We show the results in Fig. 3.

In the case of the cylinder we took the order parameter to be a piecewise constant function of the radius and transformed the integral equation to a matrix equation where the elements of the matrix were given as integrals of the kernel over squares in the (r, r') plane. To speed up the calculation we used various approximations for the kernel, such as the slab kernel for large and roughly equal r and r', or the asymptotic form for $r' \gg r$, which depends on r' only. Those elements containing the singular point $r = r'$ we handled either with the bulk transition temperature sum rule (which states that the kernel integrated over one of its variables gives a constant) or using the slab kernel for $r = r'$ large. The initially heavily approximated kernel was calculated exactly for a growing number of squares until the results no longer changed. The full details of the calculation can be found in Ref. 7. The transition temperature for an arbitrary radius is depicted in Fig. 2.

ACKNOWLEDGMENT

One of us (D.R.) thanks NORDITA for sponsoring his stay at the Helsinki University of Technology and the Institute for Theoretical Physics at the Helsinki University. This work has in part been financially supported by the Academy of Finland.

REFERENCES

1. A. J. Leggett, *Rev. Mod. Phys.* **47**, 331 (1975).
2. J. M. Dundon, D. L. Stolfa, and J. M. Goodkind, *Phys. Rev. Lett.* **30**, 843 (1973); A. I. Ahonen, M. Krusius, and M. T. Haikala, *Phys. Lett.* **47A**, 215 (1974); A. I. Ahonen, J. Kokko, O. V. Lounasmaa, M. A. Paalanen, R. C. Richardson, W. Schoepe, and Y. Takano, *Quantum Fluids and Solids*, S. B. Trickey, E. D. Adams, and J. W. Dufty, eds. (Plenum Press, New York, 1977), p. 171; A. I. Ahonen, T. A. Alvesalo, and M. C. Veuro, preprint (1978).

3. G. Barton and M. A. Moore, *J. Low Temp. Phys.* **21**, 489 (1975); L. J. Buchholtz and A. L. Fetter, *Phys. Lett. A* **58**, 93 (1976); L. J. Buchholtz and A. L. Fetter, *Phys. Rev. B* **15**, 5225 (1977); A. L. Fetter, *Phys. Rev. B* **15**, 1350 (1977); A. L. Fetter, *Phys. Rev. B* **17**, 1152 (1978); I. A. Privorotskii, *Phys. Rev. B* **12**, 4825 (1975); I. Fomin and M. Vuorio, *J. Low Temp. Phys.* **21**, 271 (1975).
4. P. G. de Gennes and D. Rainer, *Phys. Lett. A* **46**, 429 (1974); N. D. Mermin and T.-L. Ho, *Phys. Rev. Lett.* **36**, 594 (1976); P. W. Anderson and G. Toulouse, *Phys. Rev. Lett.* **38**, 508 (1977); M. G. McClure and S. Takagi, preprint (1977).
5. K. Levin and Oriol T. Valls, *Phys. Rev. B* **17**, 191 (1978).
6. V. Ambegaokar, P. G. de Gennes, and D. Rainer, *Phys. Rev. A* **9**, 2676 (1974).
7. Lars Kjäldman, Erikoistyö, Helsinki University of Technology, Espoo, Finland.